International Journal of Applied Engineering Research ISSN 0973-4562 Volume 14, Number 22 (2019) pp. 4090-4099

Effects of Hall and Heat Transfer on Peristaltic Transport of a Johnson - Segalman Fluid in a Channel

Venkateswarlu Bhajanthri[1], Dr. Ravindra[2], Prof. R. Sivaprasad[3]

[1]*Research Scholar, Department of Mathematics, S.S.B.N. Degree & P.G. College, Ananthapuramu-515001, A.P., India.*

[2]*Lecturer in Mathematics (Retired), S.S.B.N. Degree & P.G. College, Ananthapuramu-515001, A.P., India.*

[3]*Professor, Department of Mathematics, Sri Krishnadevaraya University, Ananthapuramu-515003, A.P., India.*

Abstract

In this paper, we modeled the Hall and heat transfer effects on the peristaltic flow of a Johnson-Segalman fluid in a two - dimensional channel. The flow is investigated in a wave frame of reference moving with velocity of the wave under the assumptions of long-wavelength and low-Reynolds number. A Perturbation solution for small Weissenberg number is obtained for the axial velocity, axial pressure gradient and pressure rise per one wavelength. The effects of various emerging parameters on the pressure gradient, temperature and pumping characteristics are discussed in detail.

Keywords: Hall and Heat transfer, Johnson-Segalman fluid, Peristaltic transport

1. INTRODUCTION

Despite the fact that there are a lot of models to describe non-Newtonian behavior of the fluids but in recent years, the Johnson-Segalman fluid has attained a special status, as it includes as special cases the classical Newtonian fluid and Maxwell fluid. Effects of Hall and ion-slip currents on peristaltic transport of a couple stress fluid was analyzed by [1] Abo-Eldahab et al. Elshahed and Haroun [2] have studied the peristaltic transport of Johnson-Segalman fluid under effect of a magnetic field. Gad [3] has studied the effects of Hall current on peristaltic transport with compliant walls. Peristaltic motion of a Johnson-Segalman fluid in a planar channel was investigated by Hayat [4] et al. Hayat et al. [5] have investigated the Hall effects on peristaltic flow of a Maxwell fluid in a porous medium.

Hayat et al. [6] have studied the MHD peristaltic flow of a Johnson-Segalman fluid in channel with compliant walls. It is well known that when any conductor comes into a magnetic field which in results creates a voltage, which is perpendicular to the current and field, this effect is known as Hall Effect. Nadeem and Akram [7] studied the heat transfer in a peristaltic flow of MHD fluid with partial slip. Mekheimer Elmaboud [8] investigated the influence of heat transfer and magnetic field on peristaltic transport of a Newtonian fluid in a vertical annulus. Radhakrishnamacharya and Srinivasulu [9] investigated the interaction of peristalsis and heat transfer. Vajravelu et al. [10] have investigated the peristaltic flow of a Newtonian fluid through a porous medium in a vertical annulus with heat transfer.

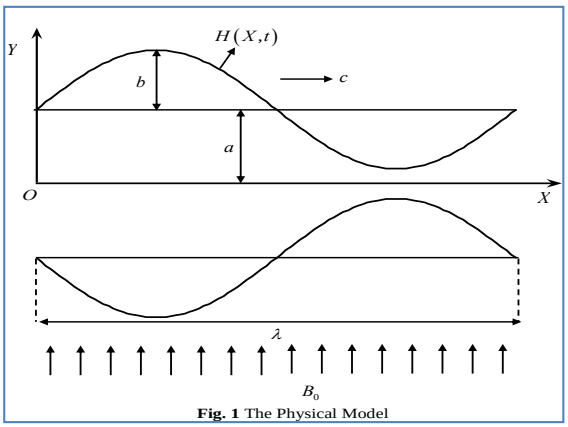

Fig. 1 The Physical Model

2. MATHEMATICAL FORMULATION

We consider an incompressible, conducting Johnson-Segalman fluid confined in a two dimensional infinite symmetric channel of width $2a$. We employ a rectangular coordinate system with X parallel to and Y normal to the channel walls. Moreover, we consider an infinite wave train traveling with velocity c along the channel walls. . A uniform magnetic field B_0 applied in the transverse direction to the flow. Fig. 1 shows the physical model of the problem. The symmetric channel walls are defined as

$$\pm H\left(X,t\right)=\pm a\pm b\cos\left[\frac{2\pi}{\lambda}\left(X-ct\right)\right] \qquad (2.1)$$

Here b is the amplitudes of the waves, t is the time and λ is the wavelength.

The constitute equation for a Johnson-Segalman fluid is given by (Johnson et al., 1977)

$$\tau=2\mu D+S \qquad (2.2)$$

$$S+m\left[\frac{dS}{dt}+S\left(W-eD\right)+\left(W-eD\right)^{T}S\right]=2\eta D \quad (2.3)$$

$$D=\frac{1}{2}\left[L+L^{T}\right],\quad W=\frac{1}{2}\left[L-L^{T}\right],\quad L=\operatorname{grad}V \quad (2.4)$$

where τ is the extra stress tensor, μ and η are the dynamic viscosities, m is the relaxation time , e is the slip parameter and the respective symmetric and D and W are skew symmetric part of the velocity gradient. Note that, our model reduces to the Maxwell fluid model for $e=1$ and $\mu=0$, and for $m=0=\mu$, it reduces to the Newtonian fluid model.

The velocity for unsteady two-dimensional flows is defined as

$$V=\left[U\left(X,Y,t\right),V\left(X,Y,t\right),0\right] \quad (2.5)$$

In the fixed frame $\left(X,Y\right)$ the motion is unsteady, while it becomes steady in the wave frame $\left(x,y\right)$. The transformation from the fixed frame of reference $\left(X,\ Y\right)$ to the wave frame of reference $\left(x,\ y\right)$ is given by

$$x=X-ct,\ y=Y,\ u=U-c,\ v=V,$$
$$p\left(x\right)=P\left(X,t\right) \quad (2.6)$$

Here *u, v* and *U, V* are the velocity components in the wave frame and in the fixed frame, respectively.

The equations governing the flow in the wave frame of reference are

$$\frac{\partial u}{\partial x}+\frac{\partial v}{\partial y}=0 \quad (2.7)$$

$$\rho\left(u\frac{\partial u}{\partial x}+v\frac{\partial u}{\partial y}\right)=-\frac{\partial p}{\partial x}+\mu\left(\frac{\partial^{2}u}{\partial x^{2}}+\frac{\partial^{2}u}{\partial y^{2}}\right)+\frac{\partial S_{xx}}{\partial x}+\frac{\partial S_{xy}}{\partial y}+\frac{\sigma B_{0}^{2}}{1+m^{2}}\left(mv-\left(u+c\right)\right) \quad (2.8)$$

$$\rho\left(u\frac{\partial v}{\partial x}+v\frac{\partial v}{\partial y}\right)=-\frac{\partial p}{\partial y}+\mu\left(\frac{\partial^{2}v}{\partial x^{2}}+\frac{\partial^{2}v}{\partial y^{2}}\right)+\frac{\partial S_{xy}}{\partial x}+\frac{\partial S_{yy}}{\partial y}-\frac{\sigma B_{0}^{2}}{1+m^{2}}\left(m\left(u+c\right)+v\right) \quad (2.9)$$

$$2\eta\frac{\partial u}{\partial x}=S_{xx}+m\left(u\frac{\partial}{\partial x}+v\frac{\partial}{\partial y}\right)S_{xx}-2emS_{xx}\frac{\partial u}{\partial x}+m\left[\left(1-e\right)\frac{\partial v}{\partial x}-\left(1+e\right)\frac{\partial u}{\partial y}\right]S_{xy} \quad (2.10)$$

$$\eta\left(\frac{\partial u}{\partial y}+\frac{\partial v}{\partial x}\right)=S_{xy}+m\left(u\frac{\partial}{\partial x}+v\frac{\partial}{\partial y}\right)S_{xy}+\frac{m}{2}\left[\left(1-e\right)\frac{\partial u}{\partial y}-\left(1+e\right)\frac{\partial v}{\partial x}\right]S_{xx}+\frac{m}{2}\left[\left(1-e\right)\frac{\partial v}{\partial x}-\left(1+e\right)\frac{\partial u}{\partial y}\right]S_{yy} \quad (2.11)$$

$$2\eta\frac{\partial v}{\partial y}=S_{yy}+m\left(u\frac{\partial}{\partial x}+v\frac{\partial}{\partial y}\right)S_{yy}-2emS_{yy}\frac{\partial v}{\partial y}+m\left[\left(1-e\right)\frac{\partial u}{\partial y}-\left(1+e\right)\frac{\partial v}{\partial x}\right]S_{xy} \quad (2.12)$$

$$\rho\zeta\left[u\frac{\partial T}{\partial x}+v\frac{\partial T}{\partial y}\right]=k\nabla^{2}T+\mu\left\{2\left[\left(\frac{\partial u}{\partial x}\right)^{2}+\left(\frac{\partial v}{\partial y}\right)^{2}\right]+\left(\frac{\partial u}{\partial y}+\frac{\partial v}{\partial x}\right)^{2}\right\} \quad (2.13)$$

where ρ is the density, T is the temperature, , k is thermal conductivity, ζ is the specific heat at constant volume, m is the Hall parameter, μ is the viscosity of the fluid and σ is the electrical conductivity.

The dimensional boundary conditions are

$$u=-c \quad \text{at} \quad y=H \quad (2.14)$$

$$\frac{\partial u}{\partial y}=0 \quad \text{at} \quad y=0 \quad (2.15)$$

$$T=T_{1} \quad \text{at} \quad y=H \quad (2.16)$$

$$\frac{\partial T}{\partial y}=0 \quad \text{at} \quad y=0 \quad (2.17)$$

Using the following non – dimensional variables

$$\bar{x}=\frac{x}{\lambda},\ \bar{y}=\frac{y}{a},\ \bar{u}=\frac{u}{c},\ \bar{v}=\frac{v}{c},$$
$$h=\frac{H}{a},\ \bar{S}=\frac{a}{\mu c}S,\ \bar{p}=\frac{a^{2}}{\lambda\left(\mu+\eta\right)c}p,$$
$$\delta=\frac{a}{\lambda},\ \mathrm{Re}=\frac{\rho ca}{\mu},\ Wi=\frac{mc}{a},\phi=\frac{b}{a},$$
$$\theta=\frac{T-T_{0}}{T_{1}-T_{0}},\mathrm{Pr}=\frac{\rho v\zeta}{k},Ec=\frac{c^{2}}{\zeta\left(T_{1}-T_{0}\right)}, \quad (2.18)$$

into the equations (2.7) – (2.13), we have (after dropping the bars)

$$\frac{\partial u}{\partial x}+\frac{\partial v}{\partial y}=0, \tag{2.19}$$

$$\begin{aligned}&\mathrm{Re}\,\delta\left(u\frac{\partial u}{\partial x}+v\frac{\partial u}{\partial y}\right)\\&=-\left(\frac{\mu+\eta}{\mu}\right)\frac{\partial p}{\partial x}+\left(\delta^2\frac{\partial^2 u}{\partial x^2}+\frac{\partial^2 u}{\partial y^2}\right)\\&+\delta\frac{\partial S_{xx}}{\partial x}+\frac{\partial S_{xy}}{\partial y}+\frac{M^2}{1+m^2}\left(m\delta v-(u+1)\right)\end{aligned} \tag{2.20}$$

$$\begin{aligned}&\mathrm{Re}\,\delta^3\left(u\frac{\partial v}{\partial x}+v\frac{\partial v}{\partial y}\right)\\&=-\left(\frac{\mu+\eta}{\mu}\right)\frac{\partial p}{\partial y}+\delta^2\left(\delta^2\frac{\partial^2 v}{\partial x^2}+\frac{\partial^2 v}{\partial y^2}\right)\\&+\delta^2\frac{\partial S_{xy}}{\partial x}+\delta\frac{\partial S_{yy}}{\partial y}-\frac{\delta M^2}{1+m^2}\left(m(u+1)+\delta v\right)\end{aligned} \tag{2.21}$$

$$\begin{aligned}&\left(\frac{2\eta\delta}{\mu}\right)\frac{\partial u}{\partial x}=S_{xx}+Wi\delta\left(u\frac{\partial}{\partial x}+v\frac{\partial}{\partial y}\right)S_{xx}-2eWi\delta S_{xx}\frac{\partial u}{\partial x}\\&+Wi\left(\delta^2(1-e)\frac{\partial v}{\partial x}-(1+e)\frac{\partial u}{\partial y}\right)S_{xy}\end{aligned} \tag{2.22}$$

$$\begin{aligned}&\frac{\eta}{\mu}\left(\frac{\partial u}{\partial y}+\delta^2\frac{\partial v}{\partial x}\right)=S_{xy}+Wi\delta\left(u\frac{\partial}{\partial x}+v\frac{\partial}{\partial y}\right)S_{xy}\\&+\frac{Wi}{2}\left[(1-e)\frac{\partial u}{\partial y}-(1+e)\delta^2\frac{\partial v}{\partial x}\right]S_{xx}\\&+\frac{Wi}{2}\left[(1-e)\delta^2\frac{\partial v}{\partial x}-(1+e)\frac{\partial u}{\partial y}\right]S_{yy}\end{aligned} \tag{2.23}$$

$$\begin{aligned}&\left(\frac{2\eta\delta}{\mu}\right)\frac{\partial v}{\partial y}=S_{yy}+Wi\delta\left(u\frac{\partial}{\partial x}+v\frac{\partial}{\partial y}\right)S_{yy}-2eWi\delta S_{yy}\frac{\partial v}{\partial y}\\&+Wi\left((1-e)\frac{\partial u}{\partial y}-\delta^2(1+e)\frac{\partial v}{\partial x}\right)S_{xy}\end{aligned} \tag{2.24}$$

$$\begin{aligned}&\mathrm{Re}\,\delta\left[u\frac{\partial\theta}{\partial x}+v\frac{\partial\theta}{\partial y}\right]=\frac{1}{\mathrm{Pr}}\left(\delta^2\frac{\partial^2\theta}{\partial x^2}+\frac{\partial^2\theta}{\partial y^2}\right)\\&+Ec\left\{4\delta^2\left(\frac{\partial u}{\partial x}\right)^2+\left(\frac{\partial u}{\partial y}\right)^2+\delta^4\left(\frac{\partial v}{\partial x}\right)^2+2\delta^2\frac{\partial u}{\partial y}\frac{\partial v}{\partial x}\right\}\end{aligned} \tag{2.25}$$

where Da is the Darcy number, $M=aB_0\sqrt{\frac{\sigma}{\mu}}$ is the Hartmann number, Pr is the Prandtl number, Re is the Reynolds number, Ec is the Eckert number and δ is the wave number.

Under lubrication approach, neglecting the terms of order δ and Re, from Equations (2.20) , (2.21) and (2.25), we get

$$0=-\left(\frac{\mu+\eta}{\mu}\right)\frac{\partial p}{\partial x}+\frac{\partial^2 u}{\partial y^2}+\frac{\partial S_{xy}}{\partial y}-\frac{M^2}{1+m^2}(u+1) \tag{2.26}$$

$$0=-\left(\frac{\mu+\eta}{\mu}\right)\frac{\partial p}{\partial y}\qquad\Rightarrow\frac{\partial p}{\partial y}=0 \tag{2.27}$$

$$\frac{1}{\mathrm{Pr}}\left[\frac{\partial^2\theta}{\partial y^2}\right]+Ec\left[\frac{\partial u}{\partial y}\right]^2=0 \tag{2.28}$$

$$\text{where } S_{xx}=Wi(1+e)\frac{\partial u}{\partial y}S_{xy} \tag{2.29}$$

$$\frac{\eta}{\mu}\frac{\partial u}{\partial y}=S_{xy}+\frac{Wi}{2}(1-e)\frac{\partial u}{\partial y}S_{xx}-\frac{Wi}{2}(1+e)\frac{\partial u}{\partial y}S_{yy} \tag{2.30}$$

$$S_{yy}=-Wi(1-e)\frac{\partial u}{\partial y}S_{xy} \tag{2.31}$$

$$S_{xy}+Wi^2(1-e^2)\left(\frac{\partial u}{\partial y}\right)^2S_{xy}=\frac{\eta}{\mu}\frac{\partial u}{\partial y} \tag{2.32}$$

From Equation (2.27), p is a function of x only. Therefore, using Equations (2.29) – (2.32), the Equation (2.26) can be rewritten as

$$\frac{dp}{dx}=\frac{\partial^2 u}{\partial y^2}+Wi^2\alpha_1\frac{\partial}{\partial y}\left[\left(\frac{\partial u}{\partial y}\right)^3\right]-\frac{1}{\left(1+\frac{\eta}{\mu}\right)}\frac{M^2}{1+m^2}(u+1) \tag{2.33}$$

$$\text{where } \alpha_1=\frac{(e^2-1)\eta}{(\mu+\eta)}=\frac{(e^2-1)}{(\gamma+1)},\gamma=\frac{\mu}{\eta}.$$

The corresponding boundary conditions in wave frame of reference are given by

$$u=-1 \quad \text{at} \quad y=h=1+\phi\cos 2\pi x, \tag{2.34}$$

$$\frac{\partial u}{\partial y}=0 \quad \text{at} \quad y=0 \tag{2.35}$$

$$\frac{\partial \theta}{\partial y}=0 \quad \text{at} \quad y=0 \tag{2.36}$$

$$\theta=1 \quad \text{at} \quad y=h \tag{2.37}$$

The volume flow rate in a wave frame is given by

$$q=\int_0^h u dy \tag{2.38}$$

The flux at any axial station in the laboratory frame is

$$Q(x,t)=\int_0^h (u+1)dy=q+h \tag{2.39}$$

The average volume flow rate over one wave period T (= λ/c) of the peristaltic wave is defined as

$$\overline{Q}=\frac{1}{T}\int_0^T Q dt=q+1 \tag{2.40}$$

3. SOLUTION

The Equation (2.33) is non-linear and its closed form solution is not possible. Thus, we linearize this equation in terms of Wi^2, since Wi is small for the type of flow under consideration. So we expand u, p and q as

$$u=u_0+Wi^2u_1+o\left(Wi^4\right)$$

$$\frac{dp}{dx}=\frac{dp_0}{dx}+Wi^2\frac{dp_1}{dx}+o\left(Wi^4\right)$$

$$q=q_0+Wi^2q_1+o\left(Wi^4\right) \tag{3.1}$$

Substituting the above expressions in to the Equations (2.33) and (2.28) and in to the boundary conditions (2.34) –(2.37), we obtain

3.1 Equations of order Wi^0

$$\frac{dp_0}{dx}=\frac{\partial^2 u_0}{\partial y^2}-\frac{\gamma}{(1+\gamma)}\frac{M^2}{1+m^2}(u_0+1) \tag{3.2}$$

$$\frac{1}{\Pr}\left[\frac{\partial^2\theta_0}{\partial y^2}\right]+Ec\left[\frac{\partial u_0}{\partial y}\right]^2=0 \tag{3.3}$$

The corresponding boundary conditions are

$$u_0=-1 \quad \text{at} \quad y=h, \tag{3.4}$$

$$\frac{\partial u_0}{\partial y}=0 \quad \text{at} \quad y=0. \tag{3.5}$$

$$\frac{\partial \theta_0}{\partial y}=0 \quad \text{at} \quad y=0 \tag{3.6}$$

$$\theta_0=1 \quad \text{at} \quad y=h \tag{3.7}$$

3.2 Equations of order Wi^2

$$\frac{dp_1}{dx}=\frac{\partial^2 u_1}{\partial y^2}+\alpha_1\frac{\partial}{\partial y}\left[\left(\frac{\partial u_0}{\partial y}\right)^3\right]-\frac{\gamma}{(1+\gamma)}\frac{M^2}{1+m^2}u_1 \tag{3.8}$$

$$\frac{\partial^2\theta_1}{\partial y^2}=-\Pr Ec\frac{\partial u_0}{\partial y}\frac{\partial u_1}{\partial y} \tag{3.9}$$

The corresponding boundary conditions are

$$u_1=0 \quad \text{at} \quad y=h, \tag{3.10}$$

$$\frac{\partial u_1}{\partial y}=0 \quad \text{at} \quad y=0. \tag{3.11}$$

$$\frac{\partial \theta_1}{\partial y}=0 \quad \text{at} \quad y=0 \tag{3.12}$$

$$\theta_1=0 \quad \text{at} \quad y=h \tag{3.13}$$

3.3 Solution of order Wi^0

Solving the Equation (3.2) by using the boundary conditions (3.4) and (3.5), we get

$$u_0=\frac{1}{\alpha^2}\frac{dp_0}{dx}\left[\frac{\cosh\alpha y}{\cosh\alpha h}-1\right]-1 \tag{3.14}$$

where $\alpha^2=\frac{\gamma M^2}{(1+\gamma)(1+m^2)}$. and the volume flow rate q_0 is given by

$$q_0=\int_0^h u_0 dy=\frac{1}{\alpha^3}\frac{dp_0}{dx}\left[\frac{(\sinh\alpha h-\alpha h\cosh\alpha h)}{\cosh\alpha h}\right]-h \tag{3.15}$$

From Equation (3.15), we obtain

$$\frac{dp_0}{dx}=\frac{\alpha^3\left(q_0+h\right)\cosh\alpha h}{\sinh\alpha h-\alpha h\cosh\alpha h} \tag{3.16}$$

Solving Eq. (3.3) using Eq. (3.14) and the boundary conditions (3.6) and (3.7), we obtain

$$\theta_0=1+\frac{\Pr Ec}{8\alpha^4\cosh^2\alpha h}\left(\frac{dp_0}{dx}\right)^2\left[2\alpha^2\left(y^2-h^2\right)+\cosh 2\alpha h-\cosh 2\alpha y\right] \tag{3.17}$$

3.4 Solution of order Wi^2

Solving the Eq. (3.8) by using Eq. (3.14) and the boundary conditions (3.10) and (3.11), we get

$$\begin{aligned}u_1=&\frac{1}{\alpha^2}\frac{dp_1}{dx}\left(\frac{\cosh\alpha y}{\cosh\alpha h}-1\right)\\&+\frac{3\alpha_1}{32\alpha^4}\left(\frac{dp_0}{dx}\right)^3\left(\frac{\cos h\alpha y}{\cosh^4\alpha h}\right)\left[\cosh 3\alpha h-4\alpha h\sinh\alpha h\right]\\&-\frac{3\alpha_1}{32\alpha^4}\left(\frac{dp_0}{dx}\right)^3\left(\frac{\cosh 3\alpha y-4\alpha y\sinh\alpha y}{\cosh^3\alpha h}\right)\end{aligned} \tag{3.18}$$

and the volume flow rate q_1 is given by

$$\begin{aligned}q_1=&\frac{1}{\alpha^3}\frac{dp_1}{dx}\left(\frac{\sinh\alpha h-\alpha h\cosh\alpha h}{\cosh\alpha h}\right)\\&+\frac{3\alpha_1}{2\alpha^4}\left(\frac{B}{\cosh^3\alpha h}\right)\left[\frac{\alpha^3\left(q_0+h\right)\cosh\alpha h}{\left(\sinh\alpha h-\alpha h\cosh\alpha h\right)}\right]^3\end{aligned} \tag{3.19}$$

where

$$B=\frac{\tanh\alpha h\cosh 3\alpha h}{16\alpha}-\frac{h\tanh\alpha h\sinh\alpha h}{4}-\frac{\sinh 3\alpha h}{48\alpha}+\frac{h\cosh\alpha h}{4}-\frac{\sinh\alpha h}{4\alpha}.$$

From Equation (3.19), we obtain

$$\begin{aligned}\frac{dp_1}{dx}=&\frac{q_1\alpha^3\cosh\alpha h}{\sinh\alpha h-\alpha h\cosh\alpha h}\\&-\frac{3\alpha_1\alpha^8 B}{2}\left[\frac{\left(q_0+h\right)^3\cosh\alpha h}{\left(\sinh\alpha h-\alpha h\cosh\alpha h\right)^4}\right]\end{aligned} \tag{3.20}$$

Solving Eq. (3.9) by using Eqs. (3.14), (3.18) and boundary conditions (3.12) and (3.13), we get

$$\begin{aligned}\theta_1=&\Pr EcA_4\\&-\Pr Ec\begin{Bmatrix}\frac{A_1}{8\alpha^2}\left(\cosh 2\alpha y-2\alpha^2y^2\right)-\frac{A_2}{32\alpha^2}\left(\cosh 4\alpha y-4\cosh 2\alpha y\right)\\+\frac{A_3}{4\alpha^3}\left(\alpha y\sinh 2\alpha y-\cosh 2\alpha y\right)\end{Bmatrix}\end{aligned} \tag{3.21}$$

where

$$\begin{aligned}A_1=&\frac{1}{\alpha^2\cosh^2\alpha h}\frac{dp_0}{dx}\frac{dp_1}{dx}\\&+\frac{3\alpha_1}{32\alpha^4}\left(\frac{dp_0}{dx}\right)^4\left(\frac{\cosh 3\alpha h-4\alpha h\sinh\alpha h+4\cosh\alpha h}{\cosh^5\alpha h}\right),\end{aligned}$$

$$A_2=\frac{9\alpha_1}{32\alpha^4\cosh^4\alpha h}\left(\frac{dp_0}{dx}\right)^4,\quad A_3=\frac{3\alpha_1}{16\alpha^3\cosh^4\alpha h}\left(\frac{dp_0}{dx}\right)^4 \text{ and}$$

$$A_4=\begin{Bmatrix}\frac{A_1}{8\alpha^2}\left(\cosh 2\alpha h-2\alpha^2h^2\right)-\frac{A_2}{32\alpha^2}\left(\cosh 4\alpha h-4\cosh 2\alpha h\right)\\+\frac{A_3}{4\alpha^3}\left(\alpha h\sinh 2\alpha h-\cosh 2\alpha h\right)\end{Bmatrix}.$$

Substituting Equations (3.16) and (3.20) into the second equation of (3.1) and neglecting terms greater than $O\left(W_i^2\right)$, we get

$$\begin{aligned}\frac{dp}{dx}=&\frac{\alpha^3\left(q+h\right)\cosh\alpha h}{\sinh\alpha h-\alpha h\cosh\alpha h}\\&-\frac{3\alpha_1B\alpha^8}{2}Wi^2\left[\frac{\left(q+h\right)^3\cosh\alpha h}{\left(\sinh\alpha h-\alpha h\cosh\alpha h\right)^4}\right]\end{aligned} \tag{3.22}$$

The dimensionless pressure rise per one wavelength in the wave frame is defined, respectively as

$$\Delta p=\int_0^{2\pi}\frac{dp}{dx}dx \tag{3.23}$$

where $h=1+\phi\sin 2\pi x$.

The heat transfer coefficient at the upper wall $y=h$ is defined by

$$Z=\left.\frac{\partial\theta}{\partial y}\frac{\partial h}{\partial x}\right|_{y=h}=-\left(A_5+Wi^2A_6\right)2\pi\phi\sin 2\pi x \tag{3.24}$$

where $A_5=\frac{\Pr Ec}{8\alpha^4\cosh^2\alpha h}\left(\frac{dp_0}{dx}\right)^2\left[4\alpha^2y-2\alpha\sinh 2\alpha y\right]$ and

$$A_6=-\Pr Ec\begin{Bmatrix}\frac{A_1}{4\alpha}\left(\sinh 2\alpha h-2\alpha h\right)-\frac{A_2}{8\alpha}\left(\sinh 4\alpha h-2\sinh 2\alpha h\right)\\+\frac{A_3}{4\alpha}\left(2\alpha h\cosh 2\alpha h-\sinh 2\alpha h\right)\end{Bmatrix}$$

.

Note that, as $m\to 0$, $M\to 0$, $Wi\to 0$ and $\mu\to 0$ our results coincide with the results of Shapiro et al. (1969) in the absence of heat transfer. Also, in the absence of heat transfer our results coincide with the results of Subba Narasimhudu (2017).

4. DISCUSSION OF THE RESULTS

Fig. 2 illustrates the variation of the axial pressure gradient $\frac{dp}{dx}$

with Wi for $\gamma=1, e=0.5,\ m=0.3,\ M=1,\ \phi=0.6$ and $\overline{Q}=-1$. It is found that, the axial pressure gradient $\frac{dp}{dx}$ decreases with increasing Weissenberg number Wi. The variation of the axial pressure gradient $\frac{dp}{dx}$ with γ for $e=0.5$, $Wi=0.02,\ m=0.3,\ M=1,\ \phi=0.6$ and $\overline{Q}=-1$ is shown in Fig. 3. It is noted that, the axial pressure gradient $\frac{dp}{dx}$ decreases with increasing γ. Fig. 4 shows the variation of the axial pressure gradient $\frac{dp}{dx}$ with e for $\gamma=1, Wi=0.02,\ m=0.3,\ M=1,\ \phi=0.6$ and $\overline{Q}=-1$. It is observed that, the axial pressure gradient $\frac{dp}{dx}$ increases with increasing slip parameter e. The variation of the axial pressure gradient $\frac{dp}{dx}$ with m for $\gamma=1, Wi=0.02,\ e=0.5,\ M=1,\ \phi=0.6$ and $\overline{Q}=-1$ is depicted in Fig. 5. It is observed that, the axial pressure gradient $\frac{dp}{dx}$ decreases with increasing Hall parameter m. Fig. 6 illustrates the variation of the axial pressure gradient $\frac{dp}{dx}$ with M for $\gamma=1,\ Wi=0.02,\ e=0.5,\ m=0.3,\ \phi=0.6$ and $\overline{Q}=-1$. It is observed that, the axial pressure gradient $\frac{dp}{dx}$ increases with increasing Hartmann number M. The variation of the axial pressure gradient $\frac{dp}{dx}$ with ϕ for $\gamma=1, Wi=0.02,\ e=0.5,\ m=0.3,\ M=1$ and $\overline{Q}=-1$ is represented In Fig. 7. It is observed that, the axial pressure gradient $\frac{dp}{dx}$ increases with increasing amplitude ratio ϕ. Fig. 8 shows the variation of the pressure rise Δp with $\overline{Q}$ for different values of Wi with $\gamma=1,\ e=0.5,\ m=0.3,\ M=1$ and $\phi=0.6$. It is observed that, in the pumping region $(\Delta p>0)$, the $\overline{Q}$ decreases with increasing weissenberg number Wi and it increases in both the free-pumping $(\Delta p=0)$ and co-pumping $(\Delta p<0)$ regions.

The variation of the pressure rise Δp with $\overline{Q}$ for different values of γ with $e=0.5, Wi=0.05,\ m=0.3,\ M=1$ and $\phi=0.6$ is shown in Fig. 9. It is observed that, in all the pumping, free-pumping and co-pumping regions, the $\overline{Q}$ increases with increasing γ.

Fig. 10 depicts the variation of the pressure rise Δp with $\overline{Q}$ for different values of e with $\gamma=1, Wi=0.05,\ m=0.3,\ M=1$ and $\phi=0.6$. It is observed that, in the pumping region $(\Delta p>0)$ and pre-pumping $(\Delta p=0)$ region, the $\overline{Q}$ increases with increasing e, while it decreases in the co-pumping $(\Delta p<0)$ region with increasing e for the chosen $\Delta p(<0)$.

The variation of the pressure rise Δp with $\overline{Q}$ for different values of m with $\gamma=1, e=0.5$, $Wi=0.05,\ M=1$ and $\phi=0.6$ is depicted in Fig. 11. It is observed that, in the pumping region, the $\overline{Q}$ decreases with increasing m while it increases in both the free-pumping and co-pumping regions with increasing m.

Fig. 12 illustrates the variation of the pressure rise Δp with $\overline{Q}$ for different values of M with $\gamma=1, e=0.5$, $Wi=0.05, m=0.3$ and $\phi=0.6$. It is observed that, in the pumping region, the $\overline{Q}$ increases with increasing M, while it decreases in both the free-pumping and co-pumping regions with increasing M.

The variation of the pressure rise Δp with $\overline{Q}$ for different values of ϕ with $\gamma=1, e=0.5$, $Wi=0.05, m=0.3$ and $M=1$ is presented in Fig. 13. It is observed that, in the pumping region $(\Delta p>0)$ and pre-pumping $(\Delta p=0)$ region, the $\overline{Q}$ increases with increasing ϕ while it decreases in the co-pumping $(\Delta p<0)$ region with increasing ϕ for the chosen value $\Delta p(<0)$.

Fig. 14 shows the temperature profiles for different values of Wi with $\phi=0.6, m=0.3,\ \Pr Ec=1,\ x=0.5,$ $q_0=-1$, $q_1=0$, $\gamma=1,\ M=1$ and $e=0.5$. It is found that the temperature θ decreases with increasing Wi.

Temperature profiles for different values of γ with $\phi=0.6,$ $m=0.3,\ \Pr Ec=1,\ x=0.5,\ q_0=-1$, $q_1=0$, $Wi=0.02,\ M=1$ and $e=0.5$ is shown in Fig. 15. It is noted that, the temperature θ decreases with increasing γ.

Fig. 16 depicts the temperature profiles for different values of e with $\phi=0.6, m=0.3,\ \Pr Ec=1,\ x=0.5,$ $q_0=-1$, $q_1=0$, $\gamma=1,\ M=1$ and $Wi=0.02$. It is observed that, the temperature θ increases with increasing e.

Temperature profiles for different values of m with $\phi=0.6,$ $Wi=0.02,\ \Pr Ec=1,\ x=0.5,\ q_0=-1$, $q_1=0$,

$\gamma = 1,\ M = 1$ and $e = 0.5$ is depicted in Fig. 17. It is found that, the temperature θ decreases with increasing m.

Fig. 18 shows the temperature profiles for different values of M with $\phi = 0.6, m = 0.3,\ \Pr Ec = 1\ ,\ x = 0.5,$ $q_0 = -1\ , q_1 = 0\ ,\ \gamma = 1,\ Wi = 0.02$ and $e = 0.5$. It is noted that, the temperature θ increases with increasing M.

Temperature profiles for different values of $\Pr Ec$ with $\phi = 0.6, m = 0.3,\ Wi = 0.02\ ,\ x = 0.5,\ q_0 = -1\ ,$ $q_1 = 0\ ,\ \gamma = 1,\ M = 1$ and $e = 0.5$ is shown in Fig. 19. It is observed that, the temperature θ increases with increasing $\Pr Ec$.

Fig. 20 illustrates the temperature profiles for different values of ϕ with $Wi = 0.02, m = 0.3,\ \Pr Ec = 1,\ x = 0.5,$ $q_0 = -1\ , q_1 = 0\ ,\ \gamma = 1,\ M = 1$ and $e = 0.5$. It is noted that, the temperature θ increases with increasing θ.

In order to see the effects of $Wi, \gamma, e, m, M, \Pr Ec$ and ϕ on the heat transfer coefficient Z at the upper wall for $x = 0.1, q_0 = -1$ and $q_1 = 0$ we have compute numerically and are presented in Table-1. Table-1 shows that, the heat transfer coefficient Z increases with increasing $e, M, \Pr Ec$ and ϕ, while it decreases with increasing Wi, γ, m and Da.

5. CONCLUSIONS:

In this paper, we studied effects of heat and hall on the peristaltic transport of a Johnson-Segalman fluid in a two - dimensional channel under the assumptions of long-wavelength. Perturbation solution for small Weissenberg number is obtained for the axial velocity, axial pressure gradient and pressure rise per one wavelength. It is found that the pressure gradient $\frac{dp}{dx}$ decreases with increasing Wi, γ or m, whereas it increases with increasing e, M or ϕ. In the pumping region, the time averaged flux $\overline{Q}$ decreases with increasing Wi or m, whereas it increases with increasing γ, e, M or ϕ. It is observed that, the temperature θ increases with increasing the parameters $e, M, \Pr Ec$ and ϕ, while it decreases with increasing Wi, γ, m and Da. Further it is found that, the heat transfer coefficient Z increases with increasing $e, M, \Pr Ec$ and ϕ, while it decreases with increasing Wi, γ, m and Da.

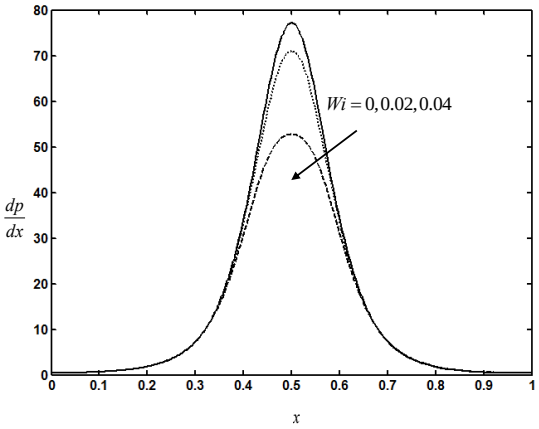

Fig. 2 The variation of the axial pressure gradient $\frac{dp}{dx}$ with Wi for $\gamma = 1, e = 0.5,$ $m = 0.3,\ M = 1,\ \phi = 0.6$ and $\overline{Q} = -1$.

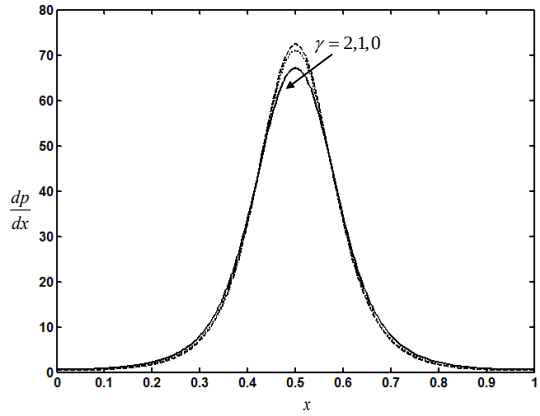

Fig. 3 The variation of the axial pressure gradient $\frac{dp}{dx}$ with γ for $e = 0.5,$ $Wi = 0.02,\ m = 0.3,\ M = 1,\ \phi = 0.6$ and $\overline{Q} = -1$.

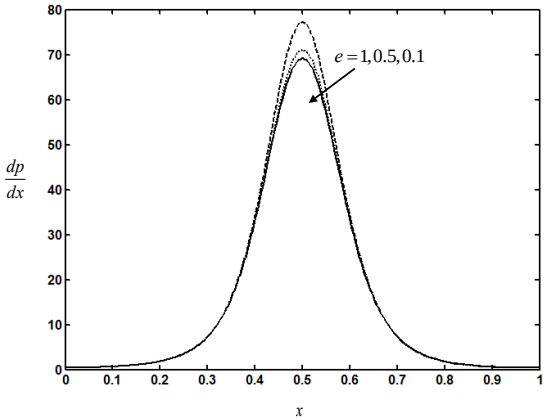

Fig. 4 The variation of the axial pressure gradient $\frac{dp}{dx}$ with e for $\gamma = 1, Wi = 0.02,$ $m = 0.3,\ M = 1,\ \phi = 0.6$ and $\overline{Q} = -1$.

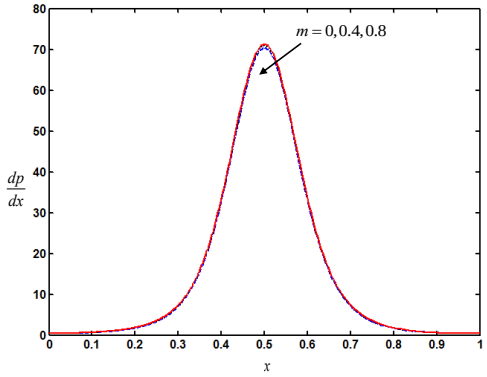

Fig. 5 The variation of the axial pressure gradient $\frac{dp}{dx}$ with m for $\gamma = 1$, $Wi = 0.02$, $e = 0.5$, $M = 1$, $\phi = 0.6$ and $\overline{Q} = -1$.

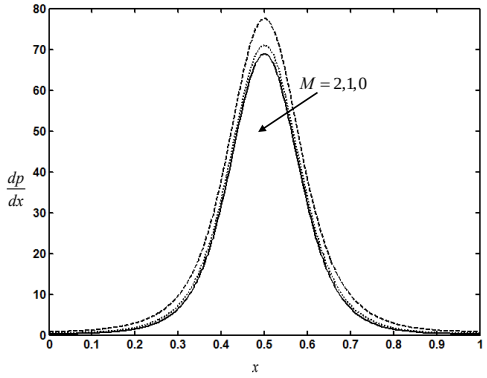

Fig. 6 The variation of the axial pressure gradient $\frac{dp}{dx}$ with M for $\gamma = 1$, $Wi = 0.02$, $e = 0.5$, $m = 0.3$, $\phi = 0.6$ and $\overline{Q} = -1$.

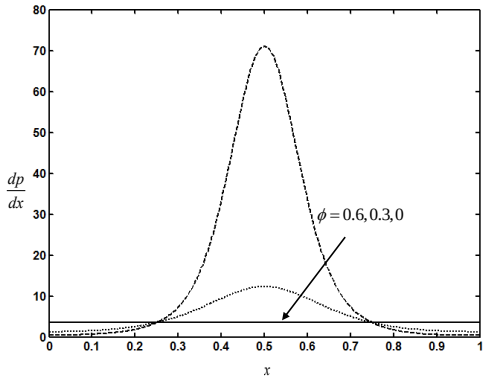

Fig. 7 The variation of the axial pressure gradient $\frac{dp}{dx}$ with ϕ for $\gamma = 1$, $Wi = 0.02$, $e = 0.5$, $m = 0.3$, $M = 1$and $\overline{Q} = -1$.

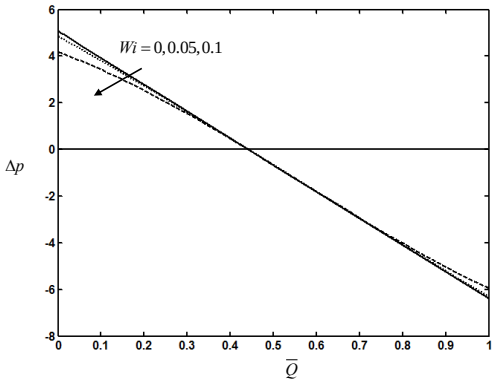

Fig. 8 The variation of the pressure rise Δp with $\overline{Q}$ for different values of Wi with $\gamma = 1$, $e = 0.5$, $m = 0.3$, $M = 1$ and $\phi = 0.6$.

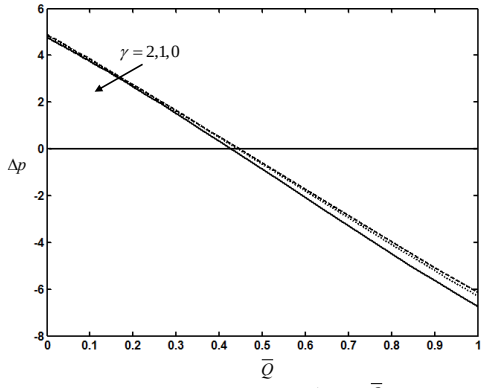

Fig. 9 The variation of the pressure rise Δp with $\overline{Q}$ for different values of γ with $e = 0.5, Wi = 0.05$, $m = 0.3$, $M = 1$ and $\phi = 0.6$.

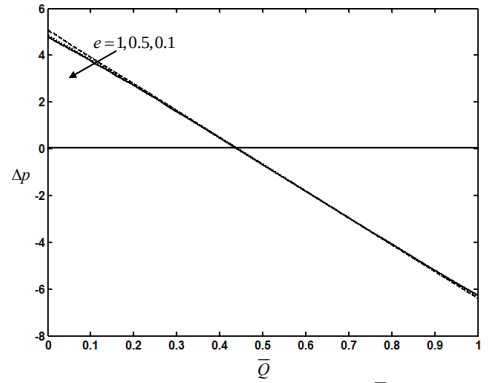

Fig. 10 The variation of the pressure rise Δp with $\overline{Q}$ for different values of e with $\gamma = 1, Wi = 0.05$, $m = 0.3$, $M = 1$ and $\phi = 0.6$.

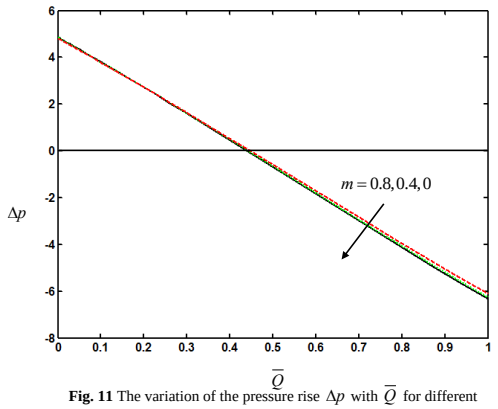

Fig. 11 The variation of the pressure rise Δp with $\overline{Q}$ for different values of m with $\gamma = 1, e = 0.5$, $Wi = 0.05$, $M = 1$ and $\phi = 0.6$.

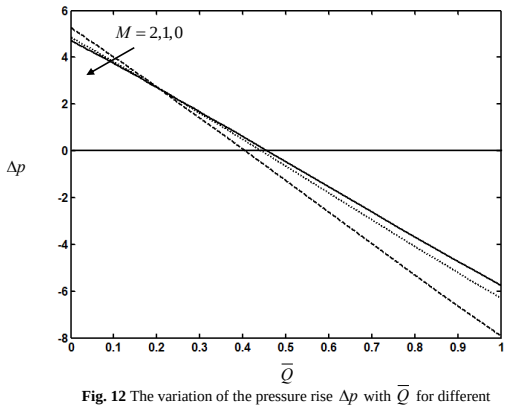

Fig. 12 The variation of the pressure rise Δp with $\overline{Q}$ for different values of M with $\gamma = 1, e = 0.5$, $Wi = 0.05, m = 0.3$ and $\phi = 0.6$.

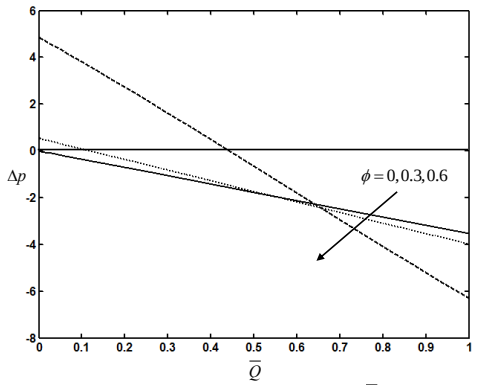

Fig. 13 The variation of the pressure rise Δp with $\overline{Q}$ for different values of ϕ with $\gamma = 1, e = 0.5$, $Wi = 0.05, m = 0.3$ and $M = 1$

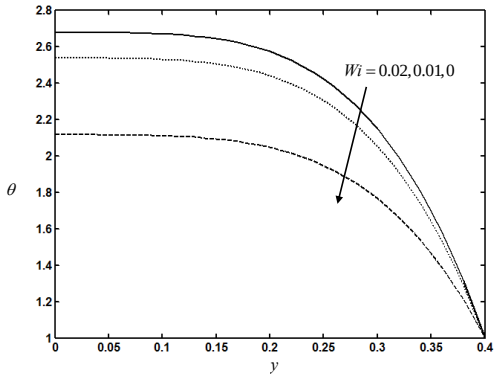

Fig. 14 Temperature profiles for different values of Wi with $\phi = 0.6$, $m = 0.3$, $\Pr Ec = 1$, $x = 0.5$, $q_0 = -1$, $q_1 = 0$, $\gamma = 1$, $M = 1$ and $e = 0.5$

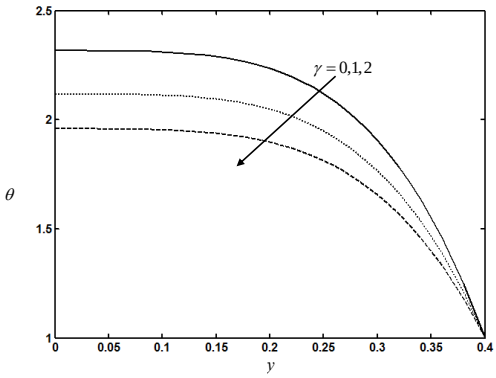

Fig. 15 Temperature profiles for different values of γ with $\phi = 0.6, m = 0.3$, $\Pr Ec = 1$, $x = 0.5$, $q_0 = -1$, $q_1 = 0$, $Wi = 0.02$, $M = 1$ and $e = 0.5$.

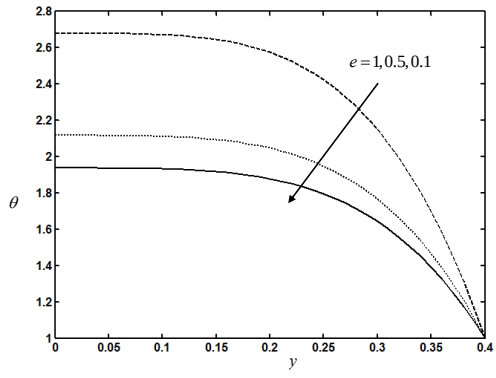

Fig. 16 Temperature profiles for different values of e with $\phi = 0.6$, $m = 0.3$, $\Pr Ec = 1$, $x = 0.5$, $q_0 = -1$, $q_1 = 0$, $\gamma = 1$, $M = 1$ and $Wi = 0.02$.

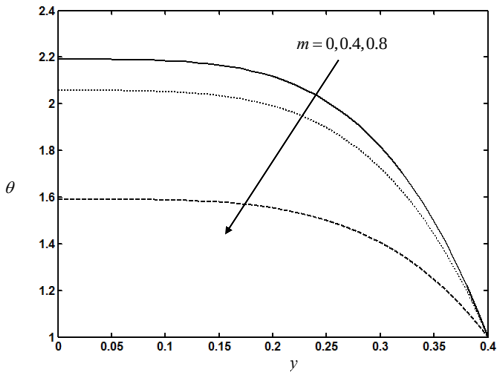

Fig. 17 Temperature profiles for different values of m with $\phi = 0.6$, $Wi = 0.02$, $\Pr Ec = 1$, $x = 0.5$, $q_0 = -1$, $q_1 = 0$, $\gamma = 1$, $M = 1$ and $e = 0.5$.

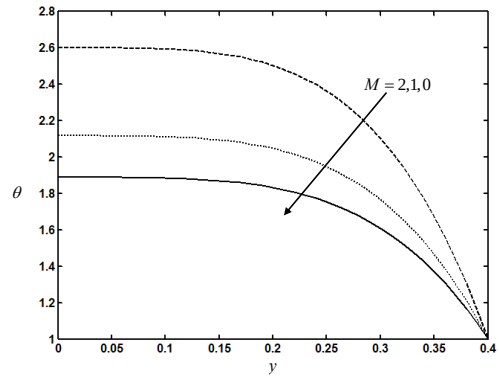

Fig. 18 Temperature profiles for different values of M with $\phi = 0.6$, $m = 0.3$, $\Pr Ec = 1$, $x = 0.5$, $q_0 = -1$, $q_1 = 0$, $\gamma = 1$, $Wi = 0.02$ and $e = 0.5$.

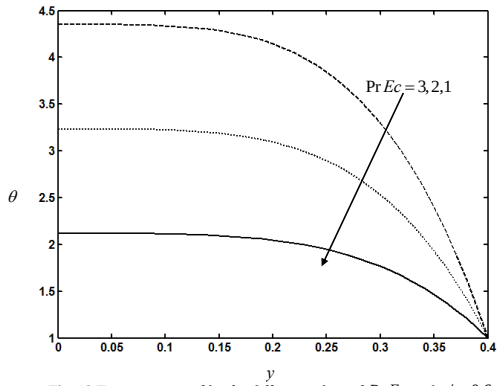

Fig. 19 Temperature profiles for different values of $\Pr Ec$ with $\phi = 0.6$, $m = 0.3$, $Wi = 0.02$, $x = 0.5$, $q_0 = -1$, $q_1 = 0$, $\gamma = 1$, $M = 1$ and $e = 0.5$.

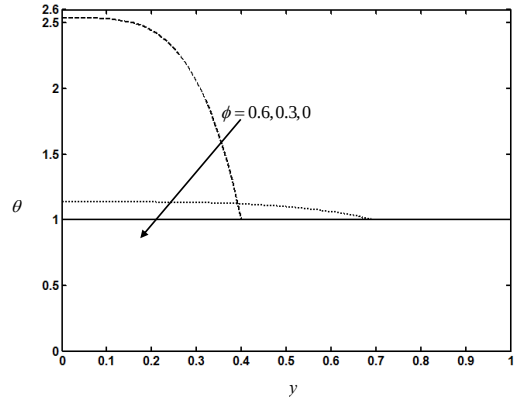

Fig. 20 Temperature profiles for different values of ϕ with $Wi = 0.02$, $m = 0.3$, $\Pr Ec = 1$, $x = 0.5$, $q_0 = -1$, $q_1 = 0$, $\gamma = 1$, $M = 1$ and $e = 0.5$.

Table 1. The effects of $\beta, \alpha, m, M, \Pr, Ec$ and ϕ on heat transfer coefficient Z at the upper wall for $x = 0.1, q_0 = -1$ and $q_1 = 0$.

Wi	γ	*e*	*m*	*M*	Pr *Ec*	ϕ	Z
0.01	1	0.5	0.3	1	1	0.6	0.4788
0.02	1	0.5	0.3	1	1	0.6	0.4787
0.01	2	0.5	0.3	1	1	0.6	0.4783
0.01	1	0.7	0.3	1	1	0.6	0.4789
0.01	1	0.5	0.6	1	1	0.6	0.4784
0.01	1	0.5	0.3	2	1	0.6	0.4887
0.01	1	0.5	0.3	1	2	0.6	0.9575
0.01	1	0.5	0.3	1	1	0.7	0.6487

REFERENCES

[1] E. M. Abo-Eldahab, E. I. Barakat, and K. I. Nowar, Effects of Hall and ion-slip currents on peristaltic transport of a couple stress fluid, International Journal of Applied Mathematics and Physics, 2 (2) (2010), 145–157.

[2] Elshahed, M. and Haroun, M. H. Peristaltic transport of Johnson-Segalman fluid under effect of a magnetic field, Math. Probl. Eng. 6(2005), 663 – 667.

[3] Gad, N.S. Effects of Hall current on peristaltic transport with compliant walls, Appl Math Comput. 235 (2014), 546–554.

[4] Hayat, T. Wang, Y., Siddiqui, A. M. and Hutter K. Peristaltic motion of a Johnson-Segalman fluid in a planar channel, Mathematical Problems in Engineering, 2003 (2003),no. 1, 1-23.

[5] Hayat, T., Ali, N. and Asghar, S. Hall effects on peristaltic flow of a Maxwell fluid in a porous medium, Physics Letters A, 363(5-6) (2007), 397–403.

[6] Hayat, T., Javed, M. and Asghar, S. MHD peristaltic motion of Johnson–Segalman fluid in a channel with compliant walls, Physics Letters A, 372 (2008), 5026–5036.

[7] Nadeem, S. and Akram, S. Heat transfer in a peristaltic flow of MHD fluid with partial slip, Commun. Nonlinear Sci. Numer. Simul. 15 (2010) 312–321.

[8] Mekheimer, Kh. S. and Abd elmaboud, Y. The influence of heat transfer and magnetic field on peristaltic transport of a Newtonian fluid in a vertical annulus: application of an endoscope, Phys. Lett. A 372 (2008) 1657–1665.

[9] Radhakrishnamacharya, G. and Srinivasulu, Ch. Influence of wall properties on peristaltic transport with heat transfer, C. R. Mecanique, 335 (2007), 369 –373.

[10] Vajravelu, K., Radhakrishnamacharya, G. and Radhakrishnamurty V. Peristaltic flow and heat transfer in a vertical porous annulus with long wave approximation. Int J Nonlinear Mech, 42(2007), 754 – 759.